Article

pubs.acs.org/Biomac

Dual-Stimuli-Sensitive Microgels as a Tool for Stimulated Spongelike Adsorption of Biomaterials for Biosensor Applications

Larisa V. Sigolaeva,*[,†] Snezhana Yu. Gladyr,[†] Arjan P. H. Gelissen,[‡] Olga Mergel,[‡] Dmitry V. Pergushov,[†] Ilya N. Kurochkin,[†] Felix A. Plamper,[‡] and Walter Richtering[‡]

[†]Department of Chemistry, M. V. Lomonosov Moscow State University, 119991 Moscow, Russia

[‡]Institute of Physical Chemistry II, RWTH Aachen University, 52056 Aachen, Germany

Supporting Information

ABSTRACT: This work examines the fabrication regime and the properties of microgel and microgel/enzyme thin films adsorbed onto conductive substrates (graphite or gold). The films were formed via two sequential steps: the adsorption of a temperature- and pH-sensitive microgel synthesized by precipitation copolymerization of *N*-isopropylacrylamide (NIPAM) and 3-(*N*,*N*-dimethylamino)propylmethacrylamide (DMAPMA) (poly(NIPAM-*co*-DMAPMA) at the pH-condition corresponding to its noncharged state (first step of adsorption), followed by the enzyme, tyrosinase, adsorption at the pH-condition when the microgel and the enzyme are oppositely charged (second step of adsorption). The stimuli-sensitive properties of poly(NIPAM-*co*-DMAPMA) microgel were characterized by potentiometric titration and dynamic light scattering (DLS) in solution as well as by atomic force microscopy (AFM) and quartz crystal microbalance with dissipation monitoring (QCM-D) at solid interface. Enhanced deposition of poly(NIPAM-*co*-DMAPMA) microgel particles was shown at elevated temperatures exceeding the volume phase transition temperature (VPTT). The subsequent electrostatic interaction of the poly(NIPAM-*co*-DMAPMA) microgel matrix with tyrosinase was examined at different adsorption regimes. A considerable increase in the amount of the adsorbed enzyme was detected when the microgel film is first brought into a collapsed state but then was allowed to interact with the enzyme at T < VPTT. Spongelike approach to enzyme adsorption was applied for modification of screen-printed graphite electrodes by poly(NIPAM-*co*-DMAPMA)/tyrosinase films and the resultant biosensors for phenol were tested amperometrically. By temperature-induced stimulating both (i) poly(NIPAM-*co*-DMAPMA) microgel adsorption at T > VPTT and (ii) following spongelike tyrosinase loading at T < VPTT, we can achieve more than 3.5-fold increase in biosensor sensitivity for phenol assay. Thus, a very simple, novel, and fast strategy for physical entrapment of biomolecules by the polymeric matrix was proposed and tested. Being based on this unique stimuli-sensitive behavior of the microgel, this stimulated spongelike adsorption provides polymer films comprising concentrated biomaterial.

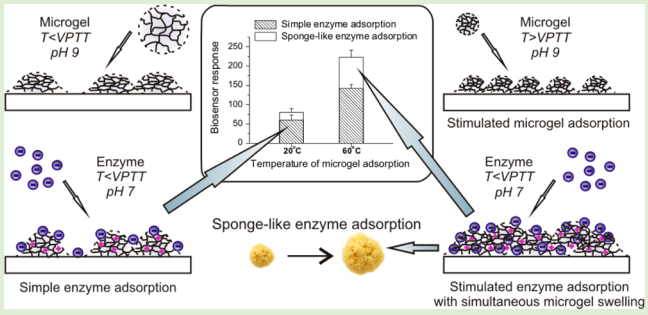

INTRODUCTION

Among different ways of immobilization of biomolecules on a solid support, a spontaneous adsorption/loading of biomolecules onto/into a host polymeric matrix represents an easy method for surface modification. Loading of biological agent(s) is usually achieved spontaneously through electrostatic, van der Waals, and/or hydrophobic interactions between the agent and the polymer matrix. Due to simplicity, this way of the interaction of biomolecules with a surface is an increasingly important challenge for a range of applications including diagnostic microarrays, biomaterials for regenerative medicine, biosensors, and drug delivery.[1−5]

Microgels like hydrogels can be considered as perfect host matrix for biomolecules, providing excellent biocompatible environment to preserve their active and functional structure.[6] Microgels based on cross-linked polymers constitute an interesting group of hydrogels since they combine properties of macrogels with typical features of colloidal systems. Typically, microgels are spherical particles with the size ranging from 50 nm up to 5 μm.

The interesting and important feature of some (micro)gel systems is stimuli-responsive behavior, which is induced by changes in the environment, such as pH, temperature, or ionic strength, leading to variations in the properties of (micro)gels, such as dimensions, structure, and interactions.[7] The numerous applications of stimuli-sensitive systems based on (micro)gels provide reversible switching between interacting and non-interacting states of biomaterial for a number of cycles (cell culture,[8] drug delivery,[9] etc.). Reversible temperature-induced change in specific enzymatic activity has also been demonstrated for (micro)gels comprising immobilized enzymes.[10−13]

Received: July 16, 2014
Revised: September 9, 2014
Published: September 11, 2014

Scheme 1. Principle of Adsorption Stimulated by pH- and Temperature-Sensitive Behavior of the Microgel[a]

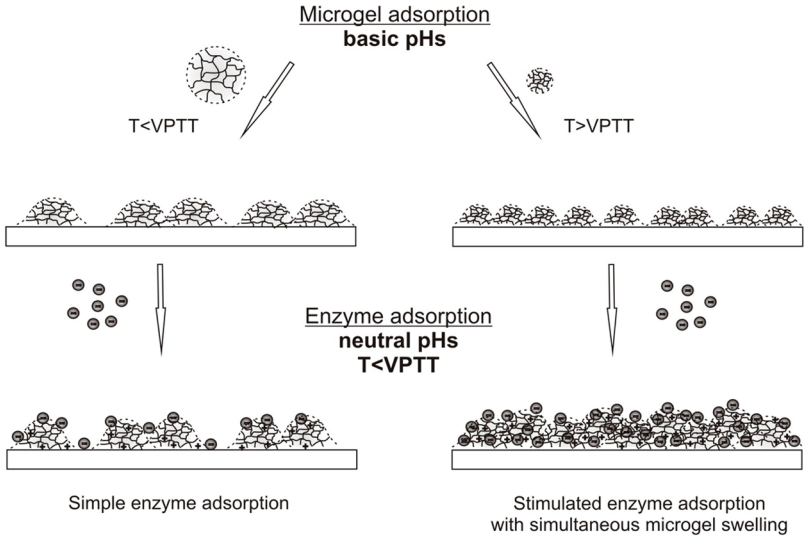

[a]The scheme describes the case when a negatively charged enzyme interacts with a cationic microgel, although one can also apply this scheme to the opposite case when a positively charged enzyme interacts with an anionic microgel.

The most investigated among stimuli-responsive microgels is poly(*N*-isopropylacrylamide) (PNIPAM) one. Heating such a gel network leads to a decrease in size of the microgel over a narrow temperature range, usually referred to as the volume phase transition temperature (VPTT), which is about 32 °C in water.[14] The collapse of the PNIPAM gel is accompanied by expelling water from its interior. In general, volume transitions in polymer gels originate from competing attractive and repulsive interactions, polymer rubber elasticity, osmotic pressure, and other forces including H-bonding, hydrophobic effects, and van der Waals forces.[15]

Usually, microgels are prepared through precipitation polymerization, by which they can be synthesized on a large scale, with good particle size control, mesh size control, and relatively facile functionalization.[16] It is possible to synthesize charged microgel particles by adding a functional comonomer during the synthesis (like DMAPMA: *N*,*N*-dimethylaminopropyl methacrylamide).[17] As soon as charged moieties are present in the polymer, charged networks can absorb more water compared to uncharged networks;[18] thereby the temperature induced collapse of PNIPAM-based microgels can be suppressed.[19]

Several groups have dealt with microgel functionalized surfaces and demonstrated that microgels retain their stimuli-responsive properties at solid interfaces if adsorbed alone[20−25] or as a component of a layer-by-layer assembly.[26−30] The volume phase transition is still fast and reversible for adsorbed microgels, but the swelling capacity decreases compared to the swelling ratio in bulk solution.[21] The temperature-dependent outer and inner structure of single microgel particles in the adsorbed state was investigated by in situ liquid-cell atomic force microscopy (AFM)[23] and by grazing incidence small-angle neutron scattering (GISANS).[31]

As a rule, the microgels studied were electrostatically adsorbed or spin-coated onto a solid support (glass, silicon wafer, gold, etc.) premodified by an anchoring polymer (like poly(ethylenimine), polyallylamine, etc.).[24,32] Densely packed thermosensitive monolayers of negatively charged P(NIPAM-*co*-acrylic acid) microgel particles were examined on poly(ethylene imine), poly(allylamine hydrochloride), and poly(diallyldimethylammonium chloride) (PDADMAC) premodified silicon wafers, depending on the pH of adsorption, silicon substrate precoating, and preparation technique.[33,34] As reported, the pH-value significantly influences the adsorption density, while the substrate surface charge is less important. Hence, the electrostatic contribution of the particle−particle interaction seems to play a more pronounced role for the adsorption density than at least the electrostatic part of the particle-surface interaction. Alternatively, loosely packed arrays of positively charged P(NIPAM-*co*-acrylamide-*co*-vinylamine) microgel particles were prepared on hydrophilic polyallylamine brush substrate via casting of microgel water dispersion with subsequent rapid evaporation of water by hot air flux.[35]

However, dual pH- and temperature-stimuli behavior would provide more possibilities for tuning the direct microgel interaction with nearly any substrate due to broad variation of not only electrostatic but also hydrophilic−hydrophobic balance. This would be a point of interest for the modification of initially hydrophobic substrates (e.g., graphite-based substrates frequently used in the field of electrochemistry and (bio)sensors). Stimuli-controlled loading of the microgel with biomaterial could also be attractive for biosensor surface design.

The idea of stimuli-induced surface modification can be described in more detail by Scheme 1. Following this scheme, it is expected that a microgel adsorbed under the appropriate conditions (in nearly noncharged state and at T > VPTT) results in effective modification of hydrophobic solid interface, which, subsequently, upon changing pH in order to charge the microgel, can bind a larger amount of oppositely charged components (biomolecules) at the subsequent adsorption stage. When biomolecules are allowed to interact with this layer of preadsorbed microgel, the temperature, at which their adsorption occurs, should preferably be ambient (25 °C) to prevent thermo-inactivation of the biomaterial. One can envisage two rather different cases of biomolecules adsorption. In the first case, they interact with the film of microgel being in its swollen state. Mainly "surface" distribution of biomolecules on the microgel film is expected then. In the second case, when

dx.doi.org/10.1021/bm5010349 | *Biomacromolecules* 2014, 15, 3735−3745

biomolecules interact with the film of microgel transforming from its collapsed state to its swollen state, one can assume not only "surface" but also "depth" distribution of adsorbed biomolecules inside the microgel film. This will occur due to both interaction of biomolecules with the microgel and swelling of microgel particles at T < VPTT that take place simultaneously. It is worth noting that the term "depth" distribution means the distribution of biomolecules inside the microgel film due to their entrapment upon its swelling, accompanied by some penetration of biomolecules into microgel particles (depending on the mesh size of the microgel).[36,37]

Despite the numerous published data on the interaction of proteins and enzymes with dispersed and adsorbed microgels[38−46] and on biosensors prepared with microgels,[13,47−50] there were to the best of our knowledge no any data on such stimulated adsorption of microgels onto hydrophobic interfaces published so far. This would be highly required for modification of initially hydrophobic substrates, particularly, for graphite-based substrates/nanomaterials that are now in the forefront of scientific interest. Excluding the cases of thermally regulated uptake/release of small molecules like, e.g., doxorubicin,[51] polypeptide insulin,[52] or loading of siRNA via imbibing by lyophilized PNIPAM nanogels at room temperature,[53,54] there were not, to the best of our knowledge, any data published on thermally regulated stimulated interaction of enzymes with microgel matrix at the interface.

This paper intends to check the aforementioned model concept. We used a model cationic poly(NIPAM-*co*-DMAPMA) microgel directly interacting with graphite or gold substrates. The subsequent electrostatic interaction of poly(NIPAM-*co*-DMAPMA) microgel matrix with a model enzyme, tyrosinase, was examined as well. This system can be comprehended as an electrochemically active polymeric system due to the production of electrochemically active compounds within the array.[55] The special attention was paid to different adsorption regimes of both components. A very simple, novel, and fast strategy for immobilization of biomolecules was proposed, based on unique stimuli-sensitive behavior of microgels that provide thin polymer films comprising concentrated biomaterial.

EXPERIMENTAL SECTION

Materials. Tyrosinase (from mushroom, E.C. 1.14.18.1, activity 3900 U/mg for L-tyrosine) from Sigma was used for the preparation of biosensor surfaces. Phenol was purchased from Sigma-Aldrich. Highly oriented pyrolytic graphite (HOPG) with area of about 50 mm^2 was from NT-MDT (Zelenograd, Russia). The poly(NIPAM-*co*-DMAPMA) microgel was synthesized by precipitation polymerization according to the procedure described in detail in the Supporting Information. The comonomer 3-(*N*,*N*-dimethylamino)-propylmethacrylamide (DMAPMA) and the initiator 2,2′-azobis(2-methylpropioamidine) dihydrochloride (97% AAPH, V 50) were purchased from Sigma-Aldrich. The cross-linker *N*,*N*′-methylenebis-(acrylamide) (BIS) and the surfactant *N*-cetyl-*N*,*N*,*N*-trimethylammonium bromide (CTAB) were purchased from AppliChem, and the monomer *N*-isopropylamide (NIPAM) was received from Acros Organics. Phosphate buffer solutions (50 mM PBS with 100 mM NaCl) were prepared by mixing stock solutions of 50 mM NaH_2PO_4 with 100 mM NaCl and 50 mM Na_2HPO_4 with 100 mM NaCl to the pH value of 7.0. Tris buffer solutions (10 mM Tris) in the pH range of 7−9.5 were prepared by mixing stock solutions of 10 mM Tris and 10 mM Tris-HCl. All other chemicals were of analytical grade and used without further purification. All aqueous solutions were prepared using deionized water (18.2 MΩ) from a Millipore Milli-Q purification system that was distilled twice.

Methods. *Potentiometric Titration.* The microgel (50.6 mg) was dissolved in approximately 50 mL of Milli-Q water and transferred to a thermostated titration cell. The pH was adjusted by a 0.1 M HCl solution to approximately 3. After the solution was allowed to equilibrate for 15 min, portions of 2 μL 0.1 M NaOH were added by a Methrohm 665 autotitrator. The titration was performed at 25 °C. Conductivity and pH were measured simultaneously. The amount of incorporated amine and the degree of protonation of the microgel α were calculated from the dependence of pH on the volume of the added titrant (the inflection points on the dependence of conductivity on the volume of the added titrant indicated the limiting values of α, that is, $\alpha = 0$ and $\alpha = 1$). For the calculation of the corresponding pK_a value, the Henderson−Hasselbalch equation was used.

Dynamic Light Scattering (DLS). DLS measurements were carried out using an ALV setup equipped with 633 nm HeNe laser (JDS Uniphase, 35 mV), two avalanche photo diodes (PerkinElmer, SPCM-CD2969), a goniometer (ALV, CGS-8F), a digital Hardware correlator (ALV 5000), and light scattering electronics (ALV, LSE-5003). Measurements were recorded in pseudocross correlation mode. An external programmable thermostat (Julabo F32) and an index-match-bath filled with toluene were used to control the temperature of the sample. In all cases, the microgel solutions were diluted with 10 mM Tris (pH 7−9). Prior to any solution preparation, the buffers were filtered three times through regenerated cellulose filters (Sartorius) with a pore size of 0.2 μm. The scattering angle was varied between 30° and 150° in steps of 10°. The samples were highly diluted to avoid multiple scattering. Hydrodynamic radii were calculated applying the Stokes−Einstein equation to the second-order cumulant-fit analysis. PDI values were obtained from the second-order cumulant-fit analysis and found to be less than 0.1 in all cases, thus characterizing the poly(NIPAM-*co*-DMAPMA) microgel as a narrow-polydisperse sample.

Atomic Force Microscopy (AFM). For AFM imaging of the microgel films, the freshly cleaved HOPG was used (as slices of about 5 mm × 10 mm). The microgel particles were adsorbed onto the HOPG at a specified temperature by covering the HOPG slide by a drop of the 1 g/L dispersion of poly(NIPAM-*co*-DMAPMA) microgel in 10 mM Tris pH 9.5, followed by 30 min adsorption. After that time, the substrate was rinsed with Milli-Q water and shortly blown by a stream of air. All manipulations were carried out in a climate-controlled chamber at constantly controlled temperature (25 or 50 °C) and relative humidity of 60%. Prior to any AFM measurements, the samples were kept in a desiccator with silica gel for at least 30 min. If needed, samples were stored in the desiccator as well. AFM images were taken with a commercial atomic force microscope NT-NDT N′Tegra Prima SPM (NT-MDT, Russia) operating in semicontact mode in air using Si_3N_4 cantilevers (fpN 11S, F.V. Lukin State Research Institute for Problems in Physics, Russia) with tip curvature radius 10−25 nm, tip cone angle <22°, and resonance frequency 190−325 kHz. Each AFM result was presented as a typical image chosen on the basis of at least three uniform-sized images of 3 × 3 μm obtained from different places of each AFM sample. Images were analyzed with "Image Analysis 3" software (NT-MDT, Russia). Images substrate levels were flatten prior to analysis using the flattening function of the software. Objects' height and lateral size were measured using central cross sections taken perpendicular to the fast scan direction in order to minimize the effect of soft objects stretching by the cantilever. The height was determined relative to the substrate level and the lateral diameter of the adsorbed objects was measured at substrate level. The number of objects in each image was determined using the grain analysis function of the software. The average surface roughness (R_a) is the mean value of the surface height (z_{mean}) relative to the center plane, which is determined by equating the volumes enclosed by the image of the surface above and below the plane and given by the equation

dx.doi.org/10.1021/bm5010349 | Biomacromolecules 2014, 15, 3735−3745

$$R_a = \frac{1}{N_x N_y}\sum_{i=1}^{N_x}\sum_{j=1}^{N_y}|z(i,j) - z_{mean}|, \quad z_{mean} = \frac{1}{N_x N_y}\sum_{i=1}^{N_x}\sum_{j=1}^{N_y} z_{ij}$$

where N_x and N_y are the numbers of points on the x and y axes, respectively; $z(i,j)$ is the current point z-coordinate. The polydispersity of adsorbed objects was evaluated from lateral size distributions of objects plotted as histograms for each AFM image. Polidispersity index (PDI) was calculated as D_w/D_n, where D_w and D_n represent weight-average and number-average lateral sizes (diameters) of the objects, given by the formulas

$$D_w = \frac{\sum D_i^2 N_i}{\sum D_i N_i}, \quad D_n = \frac{\sum D_i N_i}{\sum N_i}, \quad \mathrm{PDI} = \frac{D_w}{D_n}$$

where D_i is a diameter of ith object, and N_i is the number of objects with the size D_i.

Quartz Crystal Microbalance with Dissipation Monitoring (QCM-D). The adsorption of the microgel and tyrosinase was followed in situ by QCM-D (Q-Sense, E1 system) equipped with a Q-Sense flow-through cell. The sensor crystals (Q-Sense) were gold-coated AT-cut quartz with gold-plated polished electrodes. The quartz crystals were excited at their fundamental frequency ($f_0 \approx 5$ MHz) as well as at the third, fifth, seventh, ninth, and eleventh overtones, corresponding to 15, 25, 35, 45, and 55 MHz, respectively. Before use, the crystals were cleaned according to the Q-Sense cleaning protocol by sequential ozone treatment for 10 min, then treatment by a mixture of Milli-Q/NH_4OH (25 wt % aq)/H_2O_2 (30 wt % aq) = 5:1:1 at 70 °C for 10 min, followed by rinsing with Milli-Q water, blowing by air flux, and again ozone treatment for 10 min. Each QCM-D experiment was carried out in a flow-through cell and was started from baseline recording for the 10 mM Tris at pH 9.5 and 25 °C. If necessary, the temperature was set at 50 °C, and the new baselines for frequency and dissipation were recorded due to solution viscosity change induced by a temperature shift. Then, the sample of the microgel was first adsorbed at the specified temperature (25 or 50 °C) from 1 g/L solution in 10 mM Tris at pH 9.5, followed by a washing step with the same buffer to remove any loosely attached material. After that, one temperature cycle (temperature shift between 25 and 50 °C and back) was carried out with the film of the microgel adsorbed onto the quartz crystal. Then, the temperature was set to 25 °C, and tyrosinase was immediately allowed to interact with the film of the preadsorbed microgel from a 1×10^{-5} M solution in 10 mM Tris at pH 7.0. Thereafter, an enzyme-free 10 mM Tris solution of the same pH was used to remove weakly adsorbed tyrosinase molecules. Finally, one more temperature cycle (temperature shift between 25 and 50 °C and back) was carried out with the microgel/tyrosinase film adsorbed onto sensor crystal. During each adsorption stage or temperature cycle, frequency and dissipation shifts were continuously recorded as a function of time. Frequency shifts were calculated for seventh overtone taking the difference in the values of f_7 before and after component adsorption with regard to film state at 25 °C and used for the further comparison. That is, Δf_7 value was calculated for the adsorbed material in its swollen state regardless of temperature at which material was deposited according to the simple formula $\Delta f_7 = f_{7(2)}^{25°C} - f_{7(1)}^{25°C}$, where $f_{7(1)}^{25°C}$ and $f_{7(2)}^{25°C}$ are frequency values before and after adsorption, respectively. Each experiment was performed at least twice.

Microgel-Enzyme Biosensor Film Assembly. For an electrochemical enzymatic activity assay of the polymer-enzyme films, the screen-printed electrodes (SPEs) were fabricated on poly(vinyl chloride) substrates of 0.2 mm thickness by means of conductive graphite paste (Gwent, UK) screen-printed by a semiautomated Winon machine (model WSC-160B, China) with a 200 mesh screen stencil. Each SPE consisted of a round-shaped working area (2.5 mm diameter), a conductive track (30 mm × 1.5 mm), and a square extremity (3 mm × 7 mm) for electrical contact. The SPEs were stored dry at ambient temperature until further use.

Microgel particles were adsorbed onto SPEs at a specified temperature in the range of 20−60 °C via the dip coating method by dipping the SPEs into preheated 10 g/L dispersion of poly(NIPAM-*co*-DMAPMA) microgel in 10 mM Tris of pH 9.5 for 60 min adsorption. After that time, the substrate was rinsed with Milli-Q at the same temperature at which adsorption was carried out and was very shortly (for 1−2 s) blown by a stream of air. Directly after this, tyrosinase was adsorbed in a similar way from 1×10^{-4} M solution in 10 mM Tris of pH 7.0 at 20 °C for 10 min, followed by rinsing with Milli-Q water and shortly drying with a stream of air. To prevent a loss of enzymatic activity, the SPE covered by microgel/tyrosinase films were stored at +4 °C until further use.

Electrochemical Assay. Electrochemical experiments were performed at ambient temperature in a one-compartment electrochemical cell with stirring (volume of 1 mL), using a two electrode configuration. An SPE covered by the microgel/tyrosinase film with an active surface area of 0.049 cm^2 served as the working electrode and Ag/AgCl (with length of 1 cm, diameter of 3 mm, and surface area of 1.03 cm^2) was used as a reference electrode. A micropotentiostat IPC-Micro (Kronas Ltd., Russia) used for electrochemical measurements was interfaced with PC and electrochemical parameters were controlled by micropotentiostat software. An activity of microgel/tyrosinase films was measured in 50 mM PBS with 100 mM NaCl (pH 7.0) by recording the current arising in response to the addition of standard phenol concentration (10^{-6} M of phenol in the cell). Reductive current is generated due to *o*-quinone reduction at an applied potential (−150 mV vs Ag/AgCl), and is directly proportional to the tyrosinase activity. The analytical signal of enzyme-based electrodes was determined as a value of steady-state baseline current change (the difference between an average value of steady-state baseline current before and after analyte addition). Each electrochemical result was represented as mean ± SD calculated in each case on the basis of at least three measurements obtained for at least three electrodes. The design and the measurement principle of the SPE/poly(NIPAM-*co*-DMAPMA)/tyrosinase biosensor is shown in Scheme 2.

Scheme 2. Design of SPE/Poly(NIPAM-*co*-DMAPMA)/Tyrosinase Biosensor and Principle of Phenol Assay

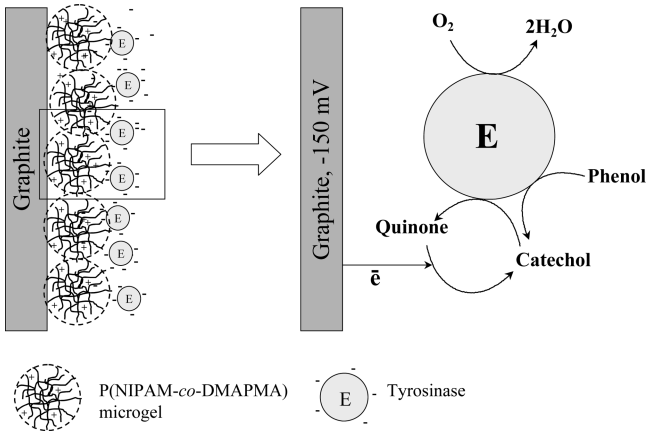

RESULTS AND DISCUSSION

A sample of poly(NIPAM-*co*-DMAPMA) microgel was synthesized in a one-step way by precipitation copolymerization of NIPAM and DMAPMA as a comonomer in the presence of cross-linking agent (BIS). The resultant microgel to be dispersed in aqueous solutions represents a colloidally stable sample of internally cross-linked polymer microparticles. These microparticles have unique combination of both thermosensitivity (imparted by NIPAM comonomer) and pH-sensitivity (imparted by DMAPMA comonomer).

The presence of DMAPMA imparts the pH-sensitivity to poly(NIPAM-*co*-DMAPMA) microgel and will provide the

dx.doi.org/10.1021/bm5010349 | Biomacromolecules 2014, 15, 3735−3745

electrostatically driven interaction with enzyme molecules. Indeed, the isoelectric point (IEP) of tyrosinase is reported to be 4.7−5.0.[56] Therefore, enzyme molecules carry a net negative charge at pH > IEP, which makes the electrostatic interaction of tyrosinase with DMAPMA groups of the microgel possible. Potentiometric titration technique allows evaluating the pH-sensitive behavior of poly(NIPAM-*co*-DMAPMA) microgel and finding the best pH conditions for both the microgel and tyrosinase adsorption. Considering α as the protonation degree of poly(NIPAM-*co*-DMAPMA) microgel and determining α = 0 and α = 1 on the potentiometric titration curve as indicated in the Experimental Section, one can plot the dependence of the protonation degree α of poly(NIPAM-*co*-DMAPMA) microgel on the pH (α vs pH) (Figure 1). According to this dependence,

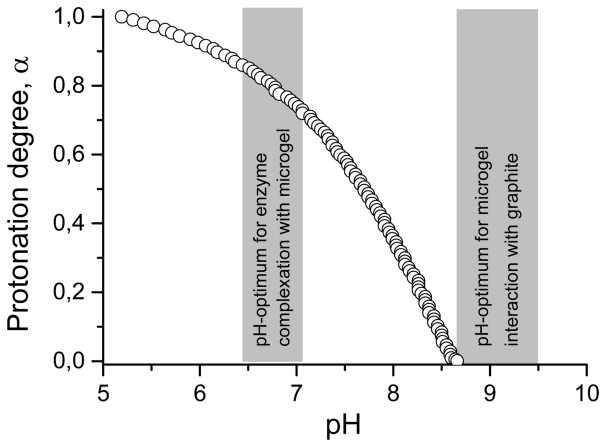

Figure 1. Dependence of the protonation degree α of poly(NIPAM-*co*-DMAPMA) microgel on the pH. The titration was started from pH of about 2.8 (preliminary adjusted by 0.1 M HCl) and was performed at 25 °C by automated stepwise addition of 2 μL of 0.1 M NaOH.

the pH-sensitive poly(NIPAM-*co*-DMAPMA) microgel undergoes a transition from the fully protonated (charged) state (α = 1) at pH of about 5.2 to the fully deprotonated (noncharged) state (α = 0) at pH of about 8.7.

On the basis of this result, we can propose pH ≥ ca. 9 (α = 0) as the optimum condition for adsorption of the microgel onto hydrophobic substrate like graphite. Alternatively, one considers the range of pHs 6.5−7 as the pH-optimum for tyrosinase adsorption that is close to the pH-optimum of its activity[49] and apparently provides sufficient amount of charges of microgel particles ($0.75 \leq \alpha \leq 0.85$) available for the interaction with enzyme molecules as well.

The amount of DMAPMA incorporated into microgel found from the data of potentiometric titration is ca. 9.3 mol %. This is close to the amount that was taken for the polymerization (DMAPMA monomer feed was 10 mol %) and is in a good agreement with the obtained ^{1}H NMR data (see Figure SI-1). In addition, the $pK_a^{app.}$ (α = 0.5) for DMAPMA in poly(NIPAM-*co*-DMAPMA) microgel was found to be 7.8 (determined according to the Henderson−Hasselbalch equation) that is close to the pK_a values for amino groups of similar structure.[26,57]

To demonstrate thermoresponsive behavior of the microgel in solution, DLS experiments were performed. Hydrodynamic radii R_h of poly(NIPAM-*co*-DMAPMA) microgel particles show a pronounced decrease with increasing temperature (Figure 2). Obviously, there is some shift of VPTT for poly(NIPAM-*co*-

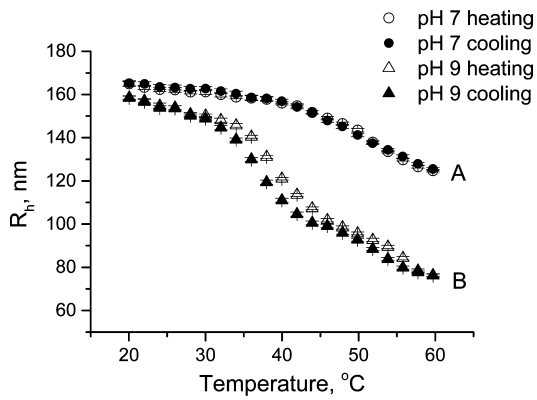

Figure 2. Temperature-dependent measurement of the hydrodynamic radius of poly(NIPAM-*co*-DMAPMA) microgel particles in 10 mM Tris of pH 7 (α = 0.85) (A) and pH 9 (α = 0) (B).

DMAPMA) microgel to the temperature range of 40−50 °C in a comparison with pure poly(*N*-isopropylacrylamide) (PNIPAM) one characterized by VPTT of about 32 °C in water.[14] The observed thermoresponsive behavior is quite reversible as can be seen from the coincidence of the corresponding R_h values in heating and cooling temperature cycles. A less pronounced decrease of R_h with temperature was found for pH 7 than for pH 9 (Figure 2). Comparing the amount of charges in poly(NIPAM-*co*-DMAPMA) microgel at pH 7 (α = 0.85) and pH 9 (α = 0), one can conclude that the electrostatic repulsion among charged groups in the microgel interior and the osmotic pressure of the counterions suppress full microgel collapse at higher levels of protonated DMAPMA groups.

The demonstrated dual-stimuli pH- and thermosensitive behavior of poly(NIPAM-*co*-DMAPMA) microgel particles in solution allows us to predict their interactions with a hydrophobic solid interface. Enhanced adsorption of microgel particles would be reasonably expected at both increased pHs and elevated temperatures. Indeed, increased adsorption of polyelectrolytes (homopolyelectrolytes and/or ionic amphiphilic (micelle-forming) diblock copolymers) onto hydrophobic interface (graphite) was achieved if their deposition was carried out in the presence of strong screening counterions for strong polyelectrolytes (charge-suppressed state)[58] or at the respective pH-value in case of weak polyelectrolytes.[59,60] Expanding this principle to microgels, we expect the highest microgel adsorption at pH in the optimum range of 9−9.5, where all DMAPMA groups are deprotonated while no notable aggregation of microgel particles still takes place. Taking into account ca. 90 mol % content of NIPAM in poly(NIPAM-*co*-DMAPMA) microgel, one could expect that even being completely deprotonated the microgel still remains very hydrophilic at temperatures below VPTT. To facilitate the adsorption of microgel particles onto hydrophobic interface, it is therefore reasonable to carry out their adsorption at T > VPTT, at which microgel particles are in their deswollen and rather hydrophobic state.

This was first examined by AFM study of the dried films formed upon the adsorption of poly(NIPAM-*co*-DMAPMA) microgel particles on a hydrophobic solid surface of HOPG at different temperature conditions (20 or 50 °C). As can be seen from the AFM images (Figure 3), the microgel film appears as uniformly distributed individual objects of spherical shape with relatively narrow size distribution characterized by PDI of 1.04, 1.02, and 1.03 for images in Figure 3A−C, respectively. Some

dx.doi.org/10.1021/bm5010349 | *Biomacromolecules* 2014, 15, 3735−3745

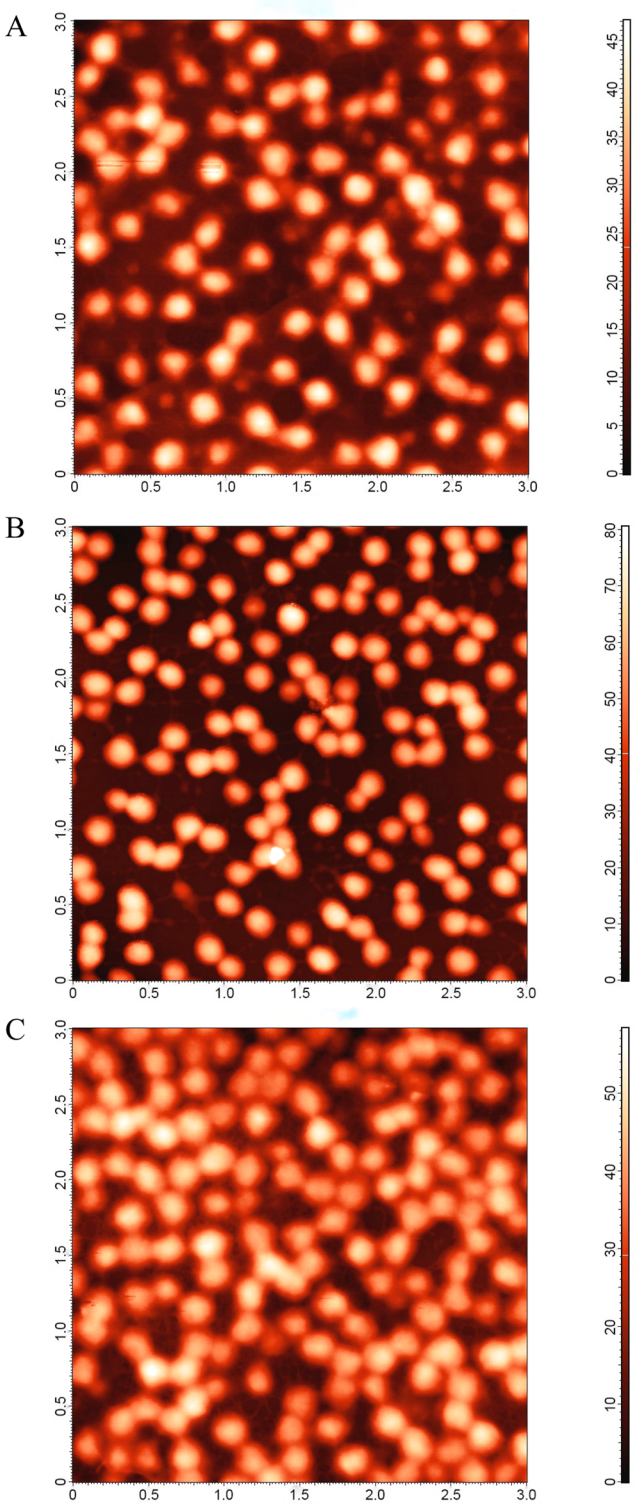

Figure 3. A series of 3 × 3 μm AFM height images of poly(NIPAM-*co*-DMAPMA) microgel particles adsorbed on HOPG at pH 9.5 from 1 g/L solutions in 10 mM Tris buffer for 30 min. Microgel particles were adsorbed at 20 °C then washed with water at 20 °C (A); microgel particles were adsorbed at 50 °C then washed with water at 50 °C (B); sample B was treated for 30 min in 10 mM Tris of pH 9.5 at 20 °C then washed with water at 20 °C (C). Images were taken in the dry state.

topographic features of AFM images of poly(NIPAM-*co*-DMAPMA) microgel particles and their swelling behavior are summarized in Table 1. Apparently, one can attribute these objects to individual microgel particles deformed to a certain extent, which is similar to other reports.[21,22,31] When these microgel particles were adsorbed at 20 °C, they appear as strongly deformed soft spheres with mean lateral diameter of 292 ± 16 nm (no tip convolution was taken into account) and mean height of 36 ± 7 nm (Figure 3A, Table 1). When microgel particles were adsorbed at 50 °C, they appeared as less deformed rigid spherical objects with mean lateral diameter of 224 ± 10 nm and mean height of 48 ± 3 nm (Figure 3B and Table 1). This corresponds well to the behavior of microgel particles in solution below and above VPPT. The most interesting conclusion drawn from the comparison of Figure 3A,B is the number of microgel particles adsorbed at different temperatures. It is clearly seen that microgel adsorption at $T >$ VPTT (Figure 3A) results in nearly 1.5-fold more material adsorbed in a comparison with the same procedure at 20 °C (cf. with Figure 3B). It is worth noting here that this kind of microgel adsorption is mostly driven by hydrophobic forces alternatively to adsorption driven by electrostatic forces described, e.g., in refs 22, 32, and 34, although both cases allow one to control the amount of the adsorbed microgel particles.

Another important feature of adsorbed poly(NIPAM-*co*-DMAPMA) microgel particles is a possibility of their postadsorption swelling. Typically, both lateral and vertical temperature-sensitive swelling/shrinkage of charged microgels on oppositely charged substrates was reported for AFM imaging taken under liquid.[23,34] In our case, the treatment of the microgel sample being initially adsorbed on HOPG at 50 °C (Figure 3B) with 10 mM Tris of pH 9.5 at 20 °C for 30 min also induces notable changes (Figure 3C). As can be seen from the AFM images taken in a dry state (Figure 3B,C), the postadsorption treatment with the same media but at reduced temperature leads to an increase of the objects diameter (that is similar to other described systems) while to a decrease of the objects height (that is probably due to AFM imaging under the air conditions) without any change in the number of adsorbed objects. Statistically treated comparison of the AFM images points out that microgel particles, when adsorbed at $T >$ VPTT and further treated with the buffer at $T <$ VPTT, come to the same state (except a higher total surface coverage) that was observed for microgel particles initially adsorbed at 20 °C (see Table 1). This allows us to conclude that poly(NIPAM-*co*-DMAPMA) microgel being strongly bound to graphite possesses thermoresponsive behavior in the adsorbed state as well. Desorption of microgel into bulk solution is not observed probably because of multipoint interaction of polymer material with solid support. It is very unlikely that it might be desorbed at least within reasonable time as polymer adsorption is typically irreversible process, even if it is not under the thermodynamically optimal state.

Thus, we can demonstrate that (i) increased adsorption of poly(NIPAM-*co*-DMAPMA) microgel can take place at elevated temperatures of microgel adsorption and (ii) microgel particles in their adsorbed state can retain their thermoresponsive behavior. Next, we examined how these features can influence the interaction of the enzyme with the film of the preadsorbed microgel. To check this, we apply a technique of QCM-D that allows simultaneous in situ measurements of a layer resonance frequency, f, and dissipation, D, at several overtones of the fundamental frequency at which both are sensitive to the mass of adsorbed material as well as its

dx.doi.org/10.1021/bm5010349 | *Biomacromolecules* 2014, 15, 3735−3745

Table 1. Topographic Features of AFM Images Taken in the Air for Poly(NIPAM-*co*-DMAPMA) Microgel Adsorbed on HOPG under Different Temperature Conditions

topographic features	temperature conditions		
	sample (1) microgel adsorbed at 20 °C	sample (2) microgel adsorbed at 50 °C	postadsorption treatment of sample (2) at 20 °C by 10 mM Tris of pH 9.0 for 30 min
number of objects per scan (mean ± SD for at least 5 scans)	101 ± 13	148 ± 23	157 ± 23
object height, nm (mean ± SD, calculated for $n > 50$ objects)	36 ± 7	48 ± 3	34 ± 3
object diameter, nm (mean ± SD, calculated for $n > 50$ objects)[a]	292 ± 16	224 ± 10	300 ± 21
surface roughness (R_a), nm (mean ± SD for at least 5 scans)	10.9 ± 2.6	17.1 ± 2.0	10.2 ± 1.4

Conditions: poly(NIPAM-*co*-DMAPMA) microgel was adsorbed onto HOPG from 1 g/L solution in 10 mM Tris of pH 9.5 at specified temperature conditions for 30 min, then washed with water at the same temperature as adsorption was carried out. [a]No tip convolution was taken into account.

viscoelastic properties. During each adsorption stage or temperature cycle, frequency and dissipation shifts were continuously recorded as a function of time.

Figure 4 illustrates a typical QCM-D experiment. Each QCM-D experiment was carried out in flow-through cell and

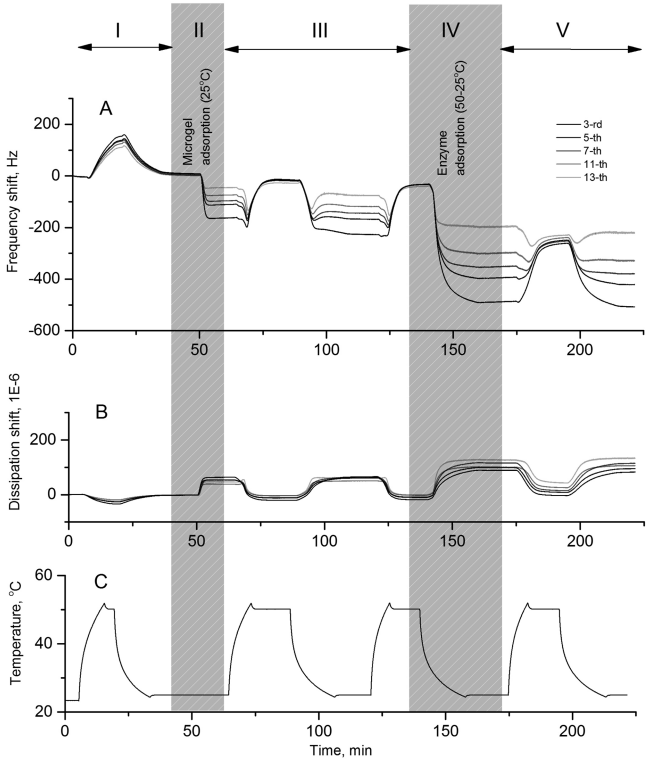

Figure 4. Frequency, f (A), dissipation, D (B), and temperature, T (C) shifts for gold-coated quartz crystal upon the consequent interaction with poly(NIPAM-*co*-DMAPMA) microgel and tyrosinase. I − temperature-induced f and D shifts for crystal in 10 mM Tris of pH 9.5 due to temperature-induced solution viscosity changes; II − microgel adsorption, 1 g/L poly(NIPAM-*co*-DMAPMA) solution in 10 mM Tris of pH 9.5; III − temperature induced swelling−deswelling behavior of the microgel film in 10 mM Tris of pH 9.5; IV − enzyme adsorption, 1.25 g/L tyrosinase solution in 10 mM Tris of pH 7.0; V − temperature induced swelling−deswelling behavior of poly(NIPAM-*co*-DMAPMA)/tyrosinase film in 10 mM Tris of pH 7.0.

was started from baseline recording for the 10 mM Tris at pH 9.5 and 25 °C. If necessary, temperature was set at 50 °C, and the new baselines for frequency and dissipation were recorded because of solution viscosity change induced by a temperature shift (Figure 4, I). Then, the sample of the microgel was first adsorbed at the specified temperature (25 °C in this experiment) from 1 g/L solution 10 mM Tris of pH 9.5, followed by a washing step with the same buffer to remove any loosely attached material (Figure 4, II). The frequency (f) and dissipation (D) changes during microgel adsorption obtained at overtone numbers of n = 3, 5, 7, 11, and 13 were recorded as a function of time. As found, microgel adsorption corresponds to a decrease of f and an increase of D with the spreading of overtones, which denotes that the mass deposited onto the quartz crystal surface exhibits viscoelastic properties. Obviously, this is because the microgel film is highly swollen and viscoelastic at T < VPTT. After that, one temperature cycle (temperature shift from 25 to 50 °C and back) was carried out with the film of the microgel adsorbed onto quartz crystal (Figure 4, III). One can see from QCM-D data that an increase of the temperature above VPTT (up to 50 °C) results in an increase in the f values. This indicates a decrease in the mass of adsorbed material due to water release (although temperature-induced changes of solution viscosity also make a contribution to these f and D shifts, cf. with Figure 4, I). Simultaneously with the decrease in f, the spreading between overtones disappeared while dissipation, D, tends to zero. All these findings point to temperature-induced change in the microgel film properties from viscoelastic to rigid, which is in agreement with the thermoresponsive feature of the microgel. Decrease of the temperature to 25 °C results in nearly complete restoring of the film water content and viscoelasticity, thereby demonstrating reversible thermoresponsive behavior of the systems and indicating absence of any desorption of the adsorbed microgel particles during temperature rearrangement of the film (Figure 4, III). As for this specific QCM-D experiment, we examined the enzyme interaction with the film of the collapsed microgel, by this reason the microgel film was equilibrated at 50 °C prior tyrosinase adsorption. Then, the temperature was set to 25 °C and the enzyme was immediately allowed to interact with the microgel film from its solution in 10 mM Tris of pH 7.0. The interaction happens together with the microgel swelling due to the simultaneous temperature decrease (Figure 4, IV). Thereafter, an enzyme-free 10 mM Tris solution of the same pH was used to remove weakly adsorbed tyrosinase molecules. Therefore, the observed shifts in f and D values are complex superpositions of (i) mass increase because of enzyme adsorption onto the microgel film; (ii) mass increase because of water uptake due to the microgel swelling; (iii) some minor changes in a water content of the microgel and viscoelastic properties of the microgel film due to change of the buffers from one with pH 9.5 to one with pH 7.0; and finally (iv) change in solution viscosity because of temperature shift. The first two among these factors provide the most considerable

dx.doi.org/10.1021/bm5010349 | *Biomacromolecules* 2014, 15, 3735−3745

contribution to a remarkable decrease in frequency and increase in dissipation observed (Figure 4, IV) with large spreading between overtones. Again, this argues for strong viscoelasticity of the resultant poly(NIPAM-*co*-DMAPMA)/tyrosinase film. Finally, one more temperature cycle (temperature shift from 25 to 50 °C and back) was carried out for poly(NIPAM-*co*-DMAPMA)/tyrosinase film (Figure 4, V) just only to show that the reversible thermoresponsive behavior of the systems is kept and no any material desorption upon temperature rearrangement of poly(NIPAM-*co*-DMAPMA)/tyrosinase film takes place.

By this way, we examined poly(NIPAM-*co*-DMAPMA) microgel adsorption onto gold-coated quartz crystals at two different temperatures: one was 25 °C < VPTT, where the microgel is adsorbed in the hydrophilic swollen state, the other was 50 °C > VPTT, when the microgel was adsorbed in its hydrophobic collapsed state. Then, we compared the tyrosinase interaction with both microgel films, provided that the microgel films were preliminarily in swollen or collapsed state depending on the temperature condition. Therefore, we examine both simple enzyme adsorption and enzyme adsorption with simultaneous microgel swelling. To be able to make some quantitative comparisons, frequency shifts were calculated for the seventh overtone taking the difference in the values of f_7 before and after component adsorption with regards to film state at 25 °C (that is, Δf_7 value was calculated for the adsorbed material in its swollen state independently of the temperature at which material was deposited). Table 2 summarizes the results for the various setups of the poly(NIPAM-*co*-DMAPMA)/tyrosinase film, the components of which were adsorbed under different temperature conditions.

Table 2. Frequency Shifts (Δf_7, Hz) Calculated for Seventh Overtone for Various Procedures of the Poly(NIPAM-*co*-DMAPMA)/Tyrosinase Film Setup

#	microgel film setup	microgel film (Δf_7, Hz)[a]	enzyme film setup	enzyme film (Δf_7, Hz)[a]
1	adsorption at 25 °C	111 ± 22	simple adsorption at 25 °C	44 ± 9
2	adsorption at 25 °C then preheating to 50 °C		adsorption at 50 °C→25 °C with simultaneous microgel swelling	135 ± 28
3	adsorption at 50 °C then precooling to 25 °C	320 ± 23	simple adsorption at 25 °C	69 ± 14
4	adsorption at 50 °C		adsorption at 50 °C→25 °C with simultaneous microgel swelling	229 ± 10

[a]Frequency shifts were calculated for seventh overtone taking the difference in the values of f_7 before and after adsorption of the components with regards to the film state at 25 °C (that is, Δf_7 value was calculated for the adsorbed material in its swollen state regardless of the temperature at which the material was deposited). Conditions: microgel adsorption, 1 g/L poly(NIPAM-*co*-DMAPMA) solution in 10 mM Tris of pH 9.5; enzyme adsorption, 10^{-5} M tyrosinase solution in 10 mM Tris of pH 7.0.

Comparing the data of Table 2 on Δf_7 (that to a first approximation can be interpreted as values proportional to masses of hydrated films adsorbed onto quartz crystal), one can see greater adsorption of the microgel induced by elevated temperature (111 ± 22 Hz for the microgel film adsorbed at 25 °C versus 320 ± 23 Hz for the microgel film adsorbed at 50 °C). This tendency is similar to the AFM imaging of poly(NIPAM-*co*-DMAPMA) microgel interacted with HOPG (Figure 3).

When both these microgel films were brought into a swollen state and then allowed to interact with tyrosinase, we see that an increased amount of the enzyme interacts with the microgel film deposited at 50 °C (cf. systems 1 and 3 in Table 2 with Δf_7 of 44 ± 9 Hz and 69 ± 14 Hz, respectively). One can explain this difference by more effective surface modification, which takes place when the microgel is deposited at T > VPTT.

However, we can considerably increase the amount of enzyme adsorbed by changing the adsorption strategy. If both microgel films were first brought into a collapsed state but then were allowed to interact with enzyme solution at T < VPTT, a considerable increase in the amount of the enzyme adsorbed can be detected (cf. systems 2 and 4 in Table 2 with Δf_7 of 135 ± 28 Hz and 229 ± 10 Hz, respectively). The most reasonable explanation of the observed effects is a simultaneous interaction of the enzyme with the microgel and swelling of microgel particles at T < VPTT that results in not only "surface" but also "depth distribution" of the adsorbed enzyme molecules inside the microgel film. Although a tyrosinase molecule has a diameter of about 10−12 nm[59] and the mean mesh size of the microgel is in a similar range,[36] one can still expect some penetration of the enzyme into them (at least into outer parts of microgel particles due to considerably larger mesh sizes caused by an inhomogeneous distribution of cross-linker moieties).[16]

Considering system 4 in Table 2 as the most effective from the point of view of enzyme loading, we now apply this method for biosensor coatings. To do this, we consequently adsorb poly(NIPAM-*co*-DMAPMA) microgel at a given temperature in a temperature range of 20−60 °C and then tyrosinase at 20 °C on the surface of screen-printed electrodes (SPEs). This allow us to assess the enzymatic activities of the resultant SPE/poly(NIPAM-*co*-DMAPMA)/tyrosinase films via amperometric assay (Figure 5). It is worth noting that poly(NIPAM-*co*-DMAPMA) microgel alone regardless of adsorption temperature has anchorage capacity with respect to tyrosinase due to electrostatic interaction (while tyrosinase, as was found, loosely adsorbs onto naked SPE and quickly washed out from it (data not shown)). However, by temperature-induced stimulating both (i) the poly(NIPAM-*co*-DMAPMA) microgel adsorption at T > VPTT and (ii) the following spongelike tyrosinase loading at T < VPTT, we can considerably increase the biosensor sensitivity for phenol assay (Figure 5A). Moreover, Figure 5B clearly demonstrates contributions of (i) and (ii) to the overall enzymatic activities of the SPE/poly(NIPAM-*co*-DMAPMA)/tyrosinase films prepared at different temperature regimes (similarly to ones described in Table 2). Thus, more than 3.5-fold effect in biosensor sensitivity increase was achieved only due to fast stimuli-induced changes of the microgel/surface and microgel/enzyme binding by tuning the hydrophobic−hydrophilic and electrostatic interactions. This demonstrates an obvious advantage of such microgel/enzyme coatings in comparison with more simple systems based on, e.g., well-known and frequently used linear PDADMAC. The latter was fabricated with limited possibility in the control of interacting forces and required a lot of optimization instead.[61,62]

CONCLUSION

We can demonstrate here that poly(NIPAM-*co*-DMAPMA) microgel adsorbed under the appropriate conditions (in

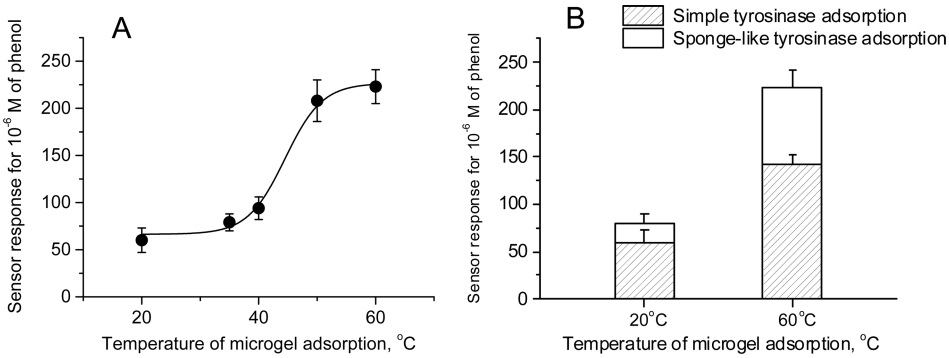

Figure 5. Enzymatic (electrochemical) activities of poly(NIPAM-*co*-DMAPMA)/tyrosinase films depending on the temperature of microgel adsorption (A) and depending on the temperature regimes of films preparation (B). Fabrication of the microgel/enzyme films: poly(NIPAM-*co*-DMAPMA) microgel adsorption onto SPE from 10 g/L solution in 10 mM Tris of pH 9.5 for 60 min in the temperature range of 20−60 °C followed by washing of surface with water at the same temperature. Then tyrosinase adsorption from 10^{-4} M solution in 10 mM Tris of pH 7.0 for 10 min at 20 °C, followed by washing with water. The electrochemical (enzymatic) activities of tyrosinase in the films were measured at ambient temperature as sensor responses for 10^{-6} M concentration of phenol. Lines through the experimentally derived data points are drawn only as a guide to the eye.

noncharged state and at T > VPTT) can result in a high amount of the adsorbed polymeric material. This itself results to binding a larger amount of tyrosinase molecules at the subsequent adsorption stage performed under the pH-condition when the microgel and the enzyme are oppositely charged. Indeed, a simple change in pH for tyrosinase adsorption leads to restoring positive charges of the microgel and makes its electrostatic interaction with the enzyme possible. Due to thermoresponsive properties of the NIPAM-containing microgel, we can additionally enhance the amount of the adsorbed enzyme due to the simultaneous interaction of tyrosinase with the adsorbed collapsed microgel and its swelling at T < VPTT. This results in not only "surface" but also "depth" distribution of enzyme molecules inside the microgel film (like a sponge soaks up liquid). Owing to fast response of poly(NIPAM-*co*-DMAPMA) microgel upon changes of external parameters, the stimulated adsorption is also fast and takes minutes. This simple playing with adsorption conditions can result in considerable concentration of both the polymeric material and biomolecules on the solid substrate. Moreover, the biomolecules fall into a favorable, highly hydrated microenvironment provided by the swollen microgel that is desirable from the point of view of stability and activity of immobilized biomaterial.

Therefore, we offer an effective way for the noncovalent and nondestructive immobilization of biomaterials. Another advantageous feature of NIPAM-containing microgels is the ease of synthesis with broad possibilities to control the mesh size, particle size, charge, and functionalization. Thus, perfectly matched pairs of microgel/biomolecules can easily be found on-demand.

This finding can have a specific practical value among the surface modification techniques applicable among biosensors for the design of, e.g., surface enhanced Raman spectroscopy (SERS) substrates, surface modification with nanomaterials, nanoparticles, quantum dots, etc.

■ ASSOCIATED CONTENT

Supporting Information

Synthesis procedure of poly(NIPAM-*co*-DMAPMA) microgel, ^{1}H NMR spectrum of the poly(NIPAM-*co*-DMAPMA) microgel. This material is available free of charge via the Internet at http://pubs.acs.org/.

■ AUTHOR INFORMATION

Corresponding Author

*E-mail: lsigolaeva@genebee.msu.ru.

Notes

The authors declare no competing financial interest.

■ ACKNOWLEDGMENTS

This research was supported by the Deutsche Forschungsgemeinschaft within SFB 985 "Funktionelle Mikrogele und Mikrogelsysteme", the Russian Foundation for Basic Research within RFBR 14-08-01108, the Lomonosov Moscow State University Program of Development, and the Lomonosov Moscow State University Post-Genomic Program. L.V.S. and D.V.P. gratefully acknowledge the SFB 985 for financial support of their research stays at the RWTH Aachen University.

■ REFERENCES

(1) Bysell, H.; Mansson, R.; Hansson, P.; Malmsten, M. Microgels and microcapsules in peptide and protein drug delivery. *Adv. Drug Delivery Rev.* **2011**, *63* (13), 1172−1185.

(2) Lu, Y.; Ballauff, M. Thermosensitive core-shell microgels: From colloidal model systems to nanoreactors. *Prog. Polym. Sci.* **2011**, *36* (6), 767−792.

(3) Malmsten, M.; Bysell, H.; Hansson, P. Biomacromolecules in microgels - Opportunities and challenges for drug delivery. *Curr. Opin. Colloid Interface Sci.* **2010**, *15* (6), 435−444.

(4) Saunders, B. R.; Laajam, N.; Daly, E.; Teow, S.; Hu, X.; Stepto, R. Microgels: From responsive polymer colloids to biomaterials. *Adv. Colloid Interface Sci.* **2009**, *147*−*48*, 251−262.

(5) Islam, M. R.; Serpe, M. J. Polyelectrolyte mediated intra and intermolecular crosslinking in microgel-based etalons for sensing protein concentration in solution. *Chem. Commun.* **2013**, *49* (26), 2646−2648.

(6) Buenger, D.; Topuz, F.; Groll, J. Hydrogels in sensing applications. *Prog. Polym. Sci.* **2012**, *37* (12), 1678−1719.

(7) Kudaibergenov, S. E.; Nuraje, N.; Khutoryanskiy, V. V. Amphoteric nano-, micro-, and macrogels, membranes, and thin films. *Soft Matter* **2012**, *8* (36), 9302−9321.

(8) Cole, M. A.; Voelcker, N. H.; Thissen, H.; Griesser, H. J. Stimuli-responsive interfaces and systems for the control of protein-surface and cell-surface interactions. *Biomaterials* **2009**, *30* (9), 1827−1850.

(9) Kabanov, A. V.; Vinogradov, S. V. Nanogels as pharmaceutical carriers: Finite networks of infinite capabilities. *Angew. Chem., Int. Ed.* **2009**, *48* (30), 5418−5429.
(10) Eremeev, N. L.; Sigolaeva, L. V.; Kazanskaya, N. F. A formal kinetic description of the temperature behavior of alpha-chymotrypsin entrapped into N-isopropylacrylamide gel. *Vestn. Mosk. Univ., Ser. 2: Khim.* **1992**, *33* (5), 511−515.
(11) Eremeev, N. L.; Sigolaeva, L. V.; Simakov, P. A.; Kazanskaya, N. F. Temperature dependences of equilibrium and kinetic constants of enzymatic-reactions during a phase-transition in a thermosensitive matrix. *Biokhimiya (Moscow)* **1995**, *60* (8), 991−999.
(12) Sigolaeva, L. V.; Eremeev, N. L.; Kazanskaya, N. F. An anomalous temperature-dependence of immobilized alpha-chymotrypsin preparations. *Bioorg. Khim.* **1994**, *20* (3), 268−273.
(13) Fernández, E.; López, D.; López-Cabarcos, E.; Mijangos, C. Viscoelastic and swelling properties of glucose oxidase loaded polyacrylamide hydrogels and the evaluation of their properties as glucose sensors. *Polymer* **2005**, *46* (7), 2211−2217.
(14) Schild, H. G. Poly (N-isopropylacrylamide) - Experiment, theory and application. *Prog. Polym. Sci.* **1992**, *17* (2), 163−249.
(15) Pelton, R. Temperature-sensitive aqueous microgels. *Adv. Colloid Interface Sci.* **2000**, *85* (1), 1−33.
(16) Pich, A.; Richtering, W. Microgels by precipitation polymerization: Synthesis, characterization, and functionalization. *Chem. Des. Responsive Microgels* **2010**, *234*, 1−37.
(17) Ogawa, K.; Nakayama, A.; Kokufuta, E. Preparation and characterization of thermosensitive polyampholyte nanogels. *Langmuir* **2003**, *19* (8), 3178−3184.
(18) Khokhlov, A. R.; Starodubtzev, S. G.; Vasilevskaya, V. V. Conformational transitions in polymer gels - Theory and experiment. *Adv. Polym. Sci.* **1993**, *109*, 123−175.
(19) Pinheiro, J. P.; Moura, L.; Fokkink, R.; Farinha, J. P. S. Preparation and characterization of low dispersity anionic multiresponsive core−shell polymer nanoparticles. *Langmuir* **2012**, *28* (13), 5802−5809.
(20) Garcia-Salinas, M. J.; Donald, A. M. Use of environmental scanning electron microscopy to image poly(N-isopropylacrylamide) microgel particles. *J. Colloid Interface Sci.* **2010**, *342* (2), 629−635.
(21) Hellweg, T.; Hofl, S.; Zitzler, L.; Herminghaus, S.; Mugele, F. Volume phase transition of "smart" microgels in bulk solution and adsorbed at an interface: A combined AFM, dynamic light, and small angle neutron scattering study. *Polymer* **2007**, *48* (1), 245−54.
(22) Schmidt, S.; Motschmann, H.; Hellweg, T.; von Klitzing, R. Thermoresponsive surfaces by spin-coating of PNIPAM-co-PAA microgels: A combined AFM and ellipsometry study. *Polymer* **2008**, *49* (3), 749−756.
(23) Horecha, M.; Senkovskyy, V.; Schneider, K.; Kiriy, A.; Stamm, M. Swelling behaviour of PNIPAM−polyisoprene core−shell microgels at surface. *Colloid Polym. Sci.* **2011**, *289* (5−6), 603−612.
(24) Hu, L.; Serpe, M. J. The influence of deposition solution pH and ionic strength on the quality of poly(N-isopropylacrylamide) microgel-based thin films and etalons. *ACS Appl. Mater. Interfaces* **2013**, *5* (22), 11977−11983.
(25) Clarke, K. C.; Lyon, L. A. Modulation of the deswelling temperature of thermoresponsive microgel films. *Langmuir* **2013**, *29* (41), 12852−12857.
(26) Gelissen, A. P. H.; Schmid, A. J.; Plamper, F. A.; Pergushov, D. V.; Richtering, W. Quaternized microgels as soft templates for polyelectrolyte layer-by-layer assemblies. *Polymer* **2014**, *55* (8), 1991−1999.
(27) Deshmukh, P. K.; Ramani, K. P.; Singh, S. S.; Tekade, A. R.; Chatap, V. K.; Patil, G. B.; Bari, S. B. Stimuli-sensitive layer-by-layer (LbL) self-assembly systems: Targeting and biosensory applications. *J. Controlled Release* **2013**, *166* (3), 294−306.
(28) Wong, J. E.; Richtering, W. Layer-by-layer assembly on stimuli-responsive microgels. *Curr. Opin. Colloid Interface Sci.* **2008**, *13* (6), 403−412.
(29) Wong, J. E.; Díez-Pascual, A. M.; Richtering, W. Layer-by-layer assembly of polyelectrolyte multilayers on thermoresponsive P(NiPAM-*co*-MAA) microgel: Effect of ionic strength and molecular weight. *Macromolecules* **2009**, *42* (4), 1229−1238.
(30) Zhang, L.; Spears, M. W.; Lyon, A. Tunable swelling and rolling of microgel membranes. *Langmuir* **2014**, *30* (26), 7628−7634.
(31) Wellert, S.; Hertle, Y.; Richter, M.; Medebach, M.; Magerl, D.; Wang, W.; Demé, B.; Radulescu, A.; Müller-Buschbaum, P.; Hellweg, T.; von Klitzing, R. Inner structure of adsorbed ionic microgel particles. *Langmuir* **2014**, *30* (24), 7168−7176.
(32) Schmidt, S.; Zeiser, M.; Hellweg, T.; Duschl, C.; Fery, A.; Möhwald, H. Adhesion and mechanical properties of PNIPAM microgel films and their potential use as switchable cell culture substrates. *Adv. Funct. Mater.* **2010**, *20* (19), 3235−3243.
(33) Schmidt, S.; Hellweg, T.; von Klitzing, R. Packing density control in P(NIPAM-*co*-AAc) microgel monolayers: Effect of surface charge, pH, and preparation technique. *Langmuir* **2008**, *24* (21), 12595−12602.
(34) Burmistrova, A.; von Klitzing, R. Control of number density and swelling/shrinking behavior of P(NIPAM-AAc) particles at solid surfaces. *J. Mater. Chem.* **2011**, *20* (17), 3502−3507.
(35) Horecha, M.; Senkovskyy, V.; Synytska, A.; Stamm, M.; Chervanyov, A. I.; Kiriy, A. Ordered surface structures from PNIPAM-based loosely packed microgel particles. *Soft Matter* **2010**, *6* (23), 5980−5992.
(36) Lehmann, S.; Seiffert, S.; Richtering, W. Spatially resolved tracer diffusion in complex responsive hydrogels. *J. Am. Chem. Soc.* **2012**, *134* (38), 15963−15969.
(37) Kleinen, J.; Klee, A.; Richtering, W. Influence of architecture on the interaction of negatively charged multisensitive poly(N-isopropylacrylamide)-*co*-methacrylic acid microgels with oppositely charged polyelectrolyte: Absorption vs adsorption. *Langmuir* **2010**, *26* (13), 11258−11265.
(38) Bysell, H.; Malmsten, M. Visualizing the interaction between poly-L-lysine and poly(acrylic acid) microgels using microscopy techniques: Effect of electrostatics and peptide size. *Langmuir* **2006**, *22* (12), 5476−5484.
(39) Dongxia, H.; Yana, L.; Qingwen, Q.; Kobayashi, T. Temperature−pH sensitivity of bovine serum albumin protein-microgels based on cross-linked poly(N-isopropylacrylamide-*co*-acrylic acid). *Colloids Surf., B* **2006**, *50* (1), 36−42.
(40) Hansson, P.; Bysell, H.; Mansson, R.; Malmsten, M. Peptide−microgel interactions in the strong coupling regime. *J. Phys. Chem. B* **2012**, *116* (35), 10964−10975.
(41) Johansson, C.; Gernandt, J.; Bradley, M.; Vincent, B.; Hansson, P. Interaction between lysozyme and colloidal poly(NIPAM-*co*-acrylic acid) microgels. *J. Colloid Interface Sci.* **2010**, *347* (2), 241−251.
(42) Welsch, N.; Dzubiella, J.; Graebert, A.; Ballauff, M. Protein binding to soft polymeric layers: A quantitative study by fluorescence spectroscopy. *Soft Matter* **2012**, *8* (48), 12043−12052.
(43) Wu, J. Y.; Liu, S. Q.; Heng, P. W. S.; Yang, Y. Y. Evaluating proteins release from, and their interactions with, thermosensitive poly(N-isopropylacrylamide) hydrogels. *J. Controlled Release* **2005**, *102* (2), 361−372.
(44) Yigit, C.; Welsch, N.; Ballauff, M.; Dzubiella, J. Protein sorption to charged microgels: Characterizing binding isotherms and driving forces. *Langmuir* **2012**, *28* (40), 14373−14385.
(45) Smith, M. H.; Lyon, L. A. Tunable encapsulation of proteins within charged microgels. *Macromolecules* **2011**, *44* (20), 8154−8160.
(46) Morisada, S.; Namazuda, K.-i.; Suzuki, S.; Kikuchi, N.; Kanda, H.; Hirokawa, Y.; Nakano, Y. Temperature-swing adsorption of proteins in water using cationic copolymer-grafted silica particles. *Ind. Eng. Chem. Res. 50*, (22), 12358−12365.
(47) González-Sánchez, M. I.; Rubio-Retama, J.; López-Cabarcos, E.; Valero, E. Development of an acetaminophen amperometric biosensor based on peroxidase entrapped in polyacrylamide microgels. *Biosens. Bioelectron.* **2011**, *26* (5), 1883−1889.
(48) Hervás Pérez, J. P.; Sánches-Paniagua López, M.; López-Cabarcos, E.; López-Ruiz, B. Amperometric tyrosinase biosensor based on polyacrylamide microgels. *Biosens. Bioelectron.* **2006**, *22* (3), 429−439.

(49) Rubio Retama, J.; Sánches-Paniagua López, M.; Hervás Pérez, J. P.; Frutos Cabanillas, G.; López-Cabarcos, E.; López-Ruiz, B. Biosensors based on acrylic microgels - A comparative study of immobilized glucose oxidase and tyrosinase. *Biosens. Bioelectron.* **2005**, *20* (11), 2268−2275.
(50) Rubio-Retama, J.; López-Cabarcos, E.; López-Ruiz, B. High stability amperometric biosensor based on enzyme entrapment in microgels. *Talanta* **2005**, *68* (1), 99−107.
(51) Serpe, M. J.; Yarmey, K. A.; Nolan, C. M.; Lyon, L. A. Doxorubicin uptake and release from microgel thin films. *Biomacromolecules* **2005**, *6* (1), 408−413.
(52) Nolan, C. M.; Serpe, M. J.; Lyon, L. A. Pulsatile release of insulin from layer-by-layer assembled microgel thin films. *Macromol. Symp.* **2005**, *227*, 285−294.
(53) Blackburn, W. H.; Dickerson, E. B.; Smith, M. H.; McDonald, J. F.; Lyon, L. A. Peptide-functionalized nanogels for targeted siRNA delivery. *Bioconjugate Chem.* **2009**, *20* (5), 960−968.
(54) Smith, M. H.; Lyon, L. A. Multifunctional nanogels for siRNA delivery. *Acc. Chem. Res.* **2012**, *45* (7), 985−993.
(55) Plamper, F. A. Changing polymer solvation by electrochemical means: Basics and applications. *Adv. Polym. Sci.* **2014**, DOI: 10.1007/1012_2014_284.
(56) Robb, D. A.; Gutteridge, S. Polypeptide composition of 2 fungal tyrosinases. *Phytochemistry* **1981**, *20* (7), 1481−1485.
(57) Thavanesan, T.; Herbert, C.; Plamper, F. A. Insight in the phase separation peculiarities of poly(dialkylaminoethyl methacrylate)s. *Langmuir* **2014**, *30* (19), 5609−5619.
(58) Gromova, M. S.; Sigolaeva, L. V.; Fastovets, M. A.; Evtushenko, E. G.; Babin, I. A.; Pergushov, D. V.; Amitonov, S. V.; Eremenko, A. V.; Kurochkin, I. N. Improved adsorption of choline oxidase on a polyelectrolyte LBL film in the presence of iodide anions. *Soft Matter* **2011**, *7* (16), 7404−7409.
(59) Sigolaeva, L. V.; Pergushov, D. V.; Synatschke, C. V.; Wolf, A.; Dewald, I.; Kurochkin, I. N.; Fery, A.; Müller, A. H. E. Co-assemblies of micelle-forming diblock copolymers and enzymes on graphite substrate for an improved design of biosensor systems. *Soft Matter* **2013**, *9* (10), 2858−2868.
(60) Sigolaeva, L. V.; Günther, U.; Pergushov, D. V.; Gladyr, S. Y.; Kurochkin, I. N.; Schacher, F. H. Sequential pH-dependent adsorption of ionic amphiphilic diblock copolymer micelles and choline oxidase onto conductive substrates: Towards the design of biosensors. *Macromol. Biosci.* **2014**, *14* (7), 1039−1051.
(61) Sigolaeva, L.; Makhaeva, G.; Rudakova, E.; Boltneva, N.; Porus, M.; Dubacheva, G.; Eremenko, A.; Kurochkin, I.; Richardson, R. J. Biosensor analysis of blood esterases for organophosphorus compounds exposure assessment: Approaches to simultaneous determination of several esterases. *Chem.-Biol. Interact.* **2010**, *187* (1−3), 312−317.
(62) Sigolaeva, L. V.; Dubacheva, G. V.; Porus, M. V.; Eremenko, A. V.; Rudakova, E. V.; Makhaeva, G. F.; Richardson, R. J.; Kurochkin, I. N. A layer-by-layer tyrosinase biosensor for assay of carboxylesterase and neuropathy target esterase activities in blood. *Anal. Methods* **2013**, *5* (16), 3872−3879.